Available online at www.sciencedirect.com

SciVerse ScienceDirect

Proceedings of the Combustion Institute 34 (2013) 547–555

Proceedings of the Combustion Institute

www.elsevier.com/locate/proci

A quantitative explanation for the apparent anomalous temperature dependence of $OH + HO_2 = H_2O + O_2$ through multi-scale modeling

Michael P. Burke *, Stephen J. Klippenstein, Lawrence B. Harding

Chemical Sciences and Engineering Division, Argonne National Laboratory, Argonne, IL 60439, USA

Available online 27 June 2012

Abstract

Kinetic models for complex chemical mechanisms are comprised of tens to thousands of reactions with rate constants informed by data from a wide variety of sources – rate constant measurements, global combustion experiments, and theoretical kinetics calculations. In order to integrate information from distinct data types in a self-consistent manner, a framework for combustion model development is presented that encapsulates behavior across a wide range of chemically relevant scales from fundamental molecular interactions to global combustion phenomena. The resulting kinetic model consists of a set of theoretical kinetics parameters (with constrained uncertainties), which are related through kinetics calculations to temperature/pressure/bath-gas-dependent rate constants (with propagated uncertainties), which in turn are related through physical models to combustion behavior (with propagated uncertainties). Direct incorporation of theory in combustion model development is expected to yield more reliable extrapolation of limited data to conditions outside the validation set, which is particularly useful for extrapolating to engine-relevant conditions where relatively limited data are available. Several key features of the approach are demonstrated for the H_2O_2 decomposition mechanism, where a number of its constituent reactions continue to have large uncertainties in their temperature and pressure dependence despite their relevance to high-pressure, low-temperature combustion of a variety of fuels. Here, we use the approach to provide a quantitative explanation for the apparent anomalous temperature dependence of $OH + HO_2 = H_2O + O_2$ – in a manner consistent with experimental data from the entire temperature range and *ab initio* transition-state theory within their associated uncertainties. Interestingly, we do find a rate minimum near 1200 K, although the temperature dependence is substantially less pronounced than previously suggested.

Keywords: Optimization; Uncertainty quantification; Multi-scale modeling; Hydrogen peroxide; *Ab initio* transition state theory

1. Introduction

As the power of scientific computing continues to grow, detailed models for complex chemical-transport phenomena play a more significant role in the design process of advanced energy conversion devices (e.g. [1]). As a result, there have been substantial research efforts devoted to the construction and further development of detailed chemical models for conventional and alternative fuels, ranging from hydrogen to green jet fuels.

* Corresponding author.
E-mail address: mpburke@anl.gov (M.P. Burke).

1540-7489/$ - see front matter © 2012 The Combustion Institute. Published by Elsevier Inc. All rights reserved.
http://dx.doi.org/10.1016/j.proci.2012.05.041

However, given the enormity of temperature/pressure/bath-gas ($T/P/M$) conditions of potential interest, kinetic models are seldom used for conditions near those of the data available for model development and validation. Examples where kinetic models exhibit significant difficulties in extrapolating to conditions outside of their validation data set are relatively commonplace, particularly for higher pressure conditions of interest to advanced engine technologies – even for relatively simple systems (e.g. [2,3]). These deficiencies highlight the need for improved techniques for combustion model development, particularly to allow more accurate extrapolation to engine-relevant conditions.

Previous strategies for combustion model development and validation have focused on identifying a set of rate parameters that describe available rate constant and combustion data. Comprehensive modeling, where the set of rate constants is validated against data spanning wide ranges of parameter space and experimental configurations, as described by Westbrook and Dryer [4], has essentially been integrated into all rigorous model development strategies. Modern mathematical extensions to model optimization largely stem from the early work of Frenklach and co-workers [5,6]. Using solution mapping techniques that related reaction rate A-factors to global combustion data, Frenklach, Wang, and co-workers optimized models for a variety of fuels (e.g. [7]). They later extended these concepts to allow uncertainty quantification and propagation that included the constraints imposed by combustion targets on reaction rate A-factors [8,9]. More recently, Turányi and co-workers have further extended these approaches to include temperature-dependent parameters from modified Arrhenius expressions in optimization and uncertainty quantification based on direct rate constant measurements and global data [10,11]. While the above-mentioned techniques take advantage of the constraints imposed by combustion targets on combinations of rate parameters (and vice versa), their reliability is limited to systems where (1) data is available to sufficiently constrain rate constants over the full range of $T/P/M$ conditions of interest and (2) full uncertainties in the relevant $T/P/M$ dependence of rate constants are considered. Extrapolation to conditions where insufficient data are available to constrain the relevant $T/P/M$ dependence of the underlying rate constants cannot be expected to be reliable in general.

In this regard, direct incorporation of theoretical kinetics calculations into combustion model development appears particularly useful – replacing dependence on rate constant fitting expressions with a physically meaningful kinetic theory. In fact, theory has often been used for extrapolation of limited rate constant experiments by adjusting uncertain theoretical kinetics parameters to reproduce direct rate constant measurements and/or global data controlled by that reaction (e.g. [12,13]). Furthermore, the accuracy of theoretical kinetics calculations has progressed to a point that it can provide useful constraints on model parameters in the same way as data from rate constant measurements and global experiments. Theoretical kinetics calculations, most importantly, impose constraints on rate constants at all $T/P/M$ conditions – essentially "filling in the gaps" in the vast $T/P/M$ parameter space and providing reliable, physically based extrapolation to conditions outside the limited experimental data set.

Here, we present an approach that integrates constraints imposed by *ab initio* kinetic theory with experimental data ranging from direct studies of elementary reactions to global studies of chemical mechanisms in a single framework. The ultimate objective of the present modeling strategy is to identify optimized values and quantified uncertainties for a set of theoretical kinetics parameters that describe the overall combustion model, constrained by data spanning fundamental molecular interactions to global combustion phenomena. An essential feature of the present multi-scale approach that enabled the conclusions below is that the system is optimized against targets from *ab initio* calculations and experimental data *simultaneously* – such that theory aids in the interpretation of global data where insufficient direct measurements are available by restricting the solution to be physically meaningful.

As a demonstration, we have implemented the approach for the H_2O_2 decomposition system. The key reactions (Table 1) have large uncertainties not only in their rate constants at specific $T/P/M$ conditions, but also in the functional form of their $T/P/M$ dependence [14] – despite their importance to predictions of high-pressure combustion phenomena for a variety of fuels (e.g. [15,16]). We focus here on $OH + HO_2 = H_2O + O_2$ (R4).

The temperature dependence of k_4 has been a persistent source of confusion and debate (see Fig. 1). The majority of experimental data are at low temperatures [17–23], where the data imply a weakly negative temperature dependence. Two sets of k_4 determinations by Troe and coworkers [24,25] suggest an uncommon and highly non-Arrhenius behavior at temperatures between 900 and 1300 K – a deep, narrow "well" in the rate constant with a minimum value nearly an order of magnitude lower than atmospheric and high-temperature values. More recent determinations by Srinivasan and Michael [26] and Hong et al. [27] in the intermediate- and high-temperature regimes exhibit only weak temperature dependence and significantly higher values than those of Troe and co-workers [24,25].

The lack of consistency in the experimental determinations and unusual apparent temperature

Table 1
List of optimization variables.

Reaction		Reaction Variables
R1	$H_2O_2(+M) = OH + OH(+M)$	$A'_{(1)}$, $n_{(1)}$, $E_{(1)}$
R2	$H_2O_2 + OH = HO_2 + H_2O$	$E^{\dagger}_{(2)}$, $\nu'_{all(2)}$, $\nu'_{tr(2)}$, $\nu'_{ss(2)}$, $\nu'_{imag(2)}$, $E_{w(2)}$, η'_{H2O2}, $\eta'_{TS(2)}$
R3	$HO_2 + HO_2 = H_2O_2 + O_2$	$E^{\dagger}_{(3)}$, $\nu'_{all(3)}$, $\nu'_{tr(3)}$, $\nu'_{ss(3)}$, $\nu'_{imag(3)}$, $E_{w(3)}$, $\eta'_{TS(3)}$
R4	$HO_2 + OH = H_2O + O_2$	$E^{\dagger}_{(4g)}$, $\nu'_{all(4)}$, $\nu'_{tr(4g)}$, $\nu'_{ss(4g)}$, $\nu'_{imag(4g)}$, $E_{w(4g)}$, $\eta'_{TS(4g)}$
		$E^{\dagger}_{(4e)}$, $\nu'_{TS(4e)}$, $\nu'_{tr(4e)}$, $\nu'_{ss(4e)}$, $\eta'_{TS(4e)}$, $f'_{VRC-TST,c(4)}$
R5	$OH + OH = O + H_2O$	$E^{\dagger}_{(5g)}$, $\nu'_{all(5)}$, $\nu'_{tr(5g)}$, $\nu'_{ss(5g)}$, $\nu'_{imag(5g)}$, $E_{w(5g)}$
		$E^{\dagger}_{(5e)}$, $\nu'_{TS(5e)}$, $\nu'_{tr(5e)}$, $\nu'_{ss(5e)}$
Global experiment		Experimental condition variables
E1-E3	Shock-heated $H_2O_2/H_2O/O_2/Ar$	T'_e, P'_e, $M'_{H2O2,o,e}$, $M'_{H2O,o,e}$, $M'_{O2,o,e}$ $e = 1\ldots3$
E4	Shock-heated $H_2O/O_2/Ar$	T'_e, P'_e, $M'_{H2O,o,e}$, $M'_{O2,o,e}$, $M'_{H,o,e}$ $e = 4$
E5-E9	Shock-heated H_2O_2/Ar	T'_e, P'_e, $M'_{H2O2,o,e}$, $\sigma'_{1,H2O2}$,$\sigma'_{2,H2O2}$,$\sigma'_{1,HO2}$, $\sigma'_{2,HO2}$ $e = 5\ldots9$

Note that $'$ indicates ln() of the quantity.

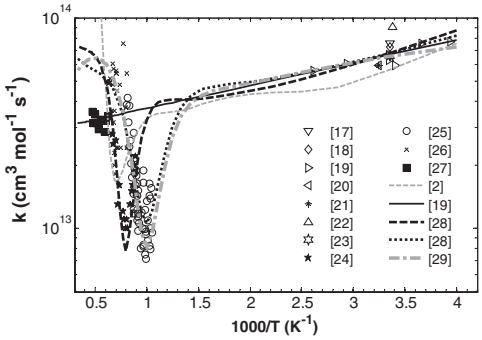

Fig. 1. Rate constants for $OH + HO_2 = H_2O + O_2$ (R4). Symbols represent experimental determinations [17–27], and lines represent proposed rate constant expressions [2,19,28,29] as indicated in the legend.

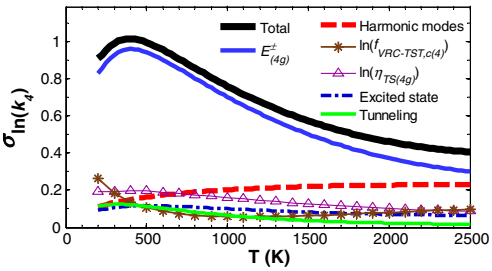

Fig. 2. Uncertainty contributions to k_4 from different classes of theoretical kinetics parameters.

dependence of k_4 has made it difficult to decide on a suitable expression for combustion modeling purposes, and a wide variety of expressions [2,28,29] have been proposed that incorporate the anomalous rate minimum. Following the recent determinations [26,27], it has been suspected [14,27,30,31] that the rate constant does not exhibit such a pronounced rate minimum, though to date it has been difficult to draw any definitive conclusions given the data at intermediate temperatures [24,25], as discussed in [14,26,27].

Below, we use the present multi-scale modeling approach to investigate this apparent inconsistency further. We discuss the general approach and specific implementation for the H_2O_2 decomposition system, demonstrate how incorporation of theory allows data at limited conditions to impose constraints on extrapolations beyond the data, and use the technique to explain experimental data across the entire temperature range [17–23,25–27] in a manner consistent with *ab initio* transition-state-theory calculations within their uncertainties. Interestingly, we do find a rate minimum for R4 near 1200 K, although the temperature dependence is substantially less pronounced than previously suggested.

2. Approach

The ultimate objective of the present modeling technique is to identify optimized values and quantified uncertainties for a set of theoretical kinetics parameters that describe the overall combustion model in a manner informed by available data from *ab initio* calculations, rate constant measurements, and global combustion measurements.

Here, we seek the set of uncertain parameters, X_j, which minimizes the least-squared error to the set of weighted equations:

$$F_i(X_j) = Y_{t,i} \pm Z_i \quad (1)$$

where $F_i(X_j)$ is the model prediction for given X_j; $Y_{t,i}$ is the target value; and the weighting factor, $Z_i = \sigma_i W_i$, is equal to the uncertainty, σ_i, times an additional data set weighting factor, W_i. Taking advantage of a "surrogate model" of the

system (as in solution mapping methods [5]) in the neighborhood of $\tilde{X}_j$,

$$F_i(X_j) \approx F_i(\tilde{X}_j) + \sum_j S_{ij}(X_j - \tilde{X}_j) \quad (2)$$

with $S_{ij} = \{dF_i/dX_j\}_{X_j=\tilde{X}_j}$, Eq. (1) can be expressed as the matrix equation:

$$\sum_j S_{ij}(X_j - \tilde{X}_j) = Y_i \pm Z_i \quad (3)$$

with $Y_i = Y_{t,i} - F_i(\tilde{X}_j)$. The optimized values and covariance matrix are calculated using a standard weighted least-squares procedure (e.g. as used in the Active Thermochemical Tables [32]). The procedure is initiated starting from the nominal values, $\tilde{X}_j^o$, and repeated in an iterative manner – solving Eq. (3) to find X_j, recalculating F_i and S_{ij} using the updated $X_j \rightarrow \tilde{X}_j$ values, and repeating – until converged. Prediction uncertainties (as in Figs. 3 and 7) were propagated using the covariance matrix. Such an approach approximates all distributions as independent and normal; it also approximates the response surface in the neighborhood of the optimized values as linear. (Uncertainty estimates that incorporate higher-order terms could be calculated [8,9,33], though they were not deemed necessary for the present study.) We have intended that uncertainties reflect two standard deviations, though the lack of specification in most studies and difficulty in estimating uncertainties in kinetics experiments (see Section 2.6 of [34]) make such a designation tentative.

As discussed below, the uncertain parameters, X_j, include theoretical kinetics parameters, rate constant parameters, and experimental conditions (initial/boundary conditions, absorption cross-sections, physical model assumptions, etc.). The targets, $Y_{t,i}$, include molecular properties from *ab initio* calculations, direct rate constant measurements, global combustion measurements, and reported values for the experimental conditions.

2.1. Target class (I): ab initio quantum chemistry calculations

Inclusion of molecular properties from *ab initio* quantum chemistry calculations (or conceivably spectroscopic measurements) is straightforward:

$$S_{ij} = \delta_{ij} \quad (4)$$

where δ_{ij} is the Kronecker delta. The system is already constrained by Eq. (4) alone if molecular property targets are used for every reaction (and if experimental condition variables are all constrained by nominal values, see below). All other data impose further constraints on the model.

2.2. Target class (II): direct rate constant measurements

Inclusion of rate constant measurements for reaction n at given $T/P/M$ conditions, $k_{t,n}(T,P,M)$, is treated here via a mapping from theoretical kinetics parameters to rate constant predictions, $k_{p,n}(T,P,M)$, employing an appropriate kinetic theory for calculating the rate constants (e.g. transition state theory, master equation simulations, quantum scattering theory):

$$S_{ij} = \frac{\partial \ln k_{p,n}(T_i,P_i,M_i)}{\partial X_j} \quad (5)$$

In practice, rather than calculating $k_{p,n}(T,P,M)$ for every $T/P/M$ condition, it was convenient to represent the $T/P/M$ dependence using a suitable parametric representation (see Supplemental data).

2.3. Target classes (III) and (IV): Global combustion measurements and experimental conditions

Inclusion of observables from global combustion experiments is treated via the mapping from theoretical kinetics parameters to rate constant predictions, discussed above, and an additional mapping from rate constants to combustion predictions, which can be written for nearly constant-temperature systems:

$$S_{ij} = \sum_n \frac{\partial F_i}{\partial \ln k_{p,n}(T_i,P_i,M_i)} \times \frac{\partial \ln k_{p,n}(T_i,P_i,M_i)}{\partial X_j}. \quad (6)$$

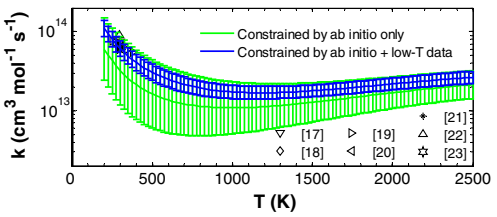

Fig. 3. Effect of inclusion of rate constant measurements at low temperatures [17–23].

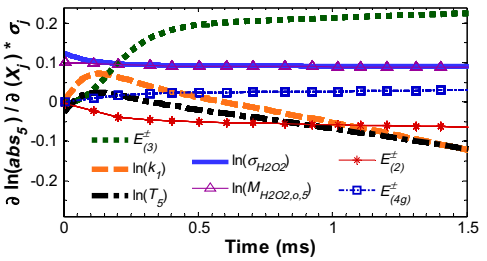

Fig. 4. Uncertainty-weighted sensitivity analysis for the absorbance time-histories of Kappel et al. [25]. (For the figure, k_1 is given an uncertainty of a factor of two, and σ_{H2O2} and σ_{HO2} are given uncertainties of 10% as reported in [25].)

Uncertainties in these targets were taken to be the root-sum-square of the uncertainty in the measurement of the observable, $\sigma_{t,i}$, and the prediction uncertainty associated with the s secondary reactions not considered in the optimization, viz.

$$\sigma_i^2 = \sigma_{t,i}^2 + \sum_{r=1}^{s} \left(\frac{\partial F_i}{\partial \ln k_r} \sigma_{\ln k,r} \right)^2 \quad (7)$$

Initial/boundary condition uncertainties can substantially affect interpretation of experimental measurements (e.g. [14,31,35–37]). Important experimental conditions were treated here as optimization variables with nominal values used as targets using the trivial mapping, Eq. (4), for two reasons: (1) to reduce systematic errors on measured observables from the same experiment caused by experimental conditions (e.g. multiple data points from time-histories in Fig. 4 below) and (2) to compile posterior statistics that can inform future choices of uncertainty bounds and characterization of potential systematic errors in experiments or model description.

3. Implementation

The approach discussed above was implemented for the H_2O_2 decomposition system. The kinetic model consisted of R1–R5 with the optimization variables listed in Table 1 and secondary reactions from the H_2/O_2 combustion model of Burke et al. [14]. The overall "model" also included optimization variables for the experimental conditions of global experiments listed in Table 1. Rate constants and brute-force sensitivity coefficients were calculated using generalized transition state theory [38] using an updated version of the VARIFLEX code [39]. For R4, which is barrierless, the two-transition-state model from Georgievskii and Klippenstein [40] was used. Combustion observables and sensitivity coefficients were calculated using homogenous, constant-pressure or constant-volume models in SENKIN [41].

For R1, Arrhenius parameters were treated as optimization variables. (The global measurements [25,36,37] used as targets sufficiently constrained k_1 over the temperature range that inclusion of *ab initio* targets was not necessary here, though we are incorporating them in our ongoing work.) For R2–R5, important uncertain parameters of the theoretical kinetics calculations were treated as optimization variables. These included: barrier heights of the transition state relative to reactants, $E^\dagger$; a scaling factor for all harmonic frequencies, ν_{all}; scaling factor for all harmonic frequencies of the (excited) transition state, ν_{TS}; scaling factor for the frequencies of transitional modes in the transition state, ν_{tr}; scaling factor for the symmetric stretching mode in the transition state, ν_{ss};

Table 2
List of optimization targets.

I. *Ab initio* calculations		Source
$E^\dagger_{(2)}$ (3 kcal); $E^\dagger_{(3)}$ (4 kcal); $E^\dagger_{(4g)}$ (2 kcal); $E^\dagger_{(4e)}$ (2 kcal); $E^\dagger_{(5g)}$ (3 kcal); $E^\dagger_{(5e)}$ (3 kcal); ν'_{all} (0.03); ν'_{TS} (0.03); ν'_{tr} (0.1); ν'_{ss} (0.18); ν'_{imag} (0.18); E_w (1 kcal); η'_{H2O2} (0.1); $\eta'_{TS(2)}$ (0.26); $\eta'_{TS(3)}$ (0.41); $\eta'_{TS(4g)}$ (0.41); $\eta'_{TS(4e)}$ (0.41); $f'_{VRC-TST,c(4)}$ (0.7)		[30]
II. Rate constant measurements		
k'_2 (see text)		[42,43]
k'_4 (see text)		[17–23,26]
k'_5 (see text)[a]		[44–48]
III. Global exp.	IV. Exp. conditions	
$M'_{OH,e}(t)$ (0.05); $M'_{H2O,e}(t)$ (0.05)	T'_e (0.01); P'_e (0.02); $M'_{H2O2,o,e}$ (0.05); $M'_{H2O,o,e}$ (0.05); $M'_{O2,o,e}$ (0.05) $e = 1\ldots3$	[36,37]
$M'_{OH,e}(t)$ (0.05)	T'_e (0.01); P'_e (0.02); $M'_{H2O,o,e}$ (0.1); $M'_{O2,o,i}$ (0.01); $M'_{H,o,e}$ (2.3) $e = 4$	[27]
$abs'_e(t)$ (0.1)	T'_e (0.02); P'_e (0.04); $M'_{H2O2,o,e}$ (0.1) $e = 5\ldots9$	
	$\sigma'_{1,H2O2}$ (0.7); $\sigma'_{2,H2O2}$ (0.3); $\sigma'_{1,HO2}$ (0.7); $\sigma'_{2,HO2}$ (0.3)	[25]

Note that $'$ indicates ln() of the quantity.
Uncertainties are listed in ().
[a] k_5 from [47,48] were derived from k_{-5} using [49]

scaling factor for the hindered rotor potential of H_2O_2, η_{H2O2}, and transition state, η_{TS}; scaling factor for the imaginary frequency in the Eckart tunneling correction, v_{imag}; the smaller of the two depths from reactants to the entrance well and products to exit well (used in the tunneling correction), E_w; and variable reaction coordinate transition state theory (VRC-TST) correction factor to account for uncertainty in the number of states in the entrance transition state, $f_{VRC-TST,c}$. Here, e and g refer to the ground and excited transition states (3A″ and 1A″ of R4; A″ and A′ of R5).

3.1. Target class (I): ab initio calculations

Molecular parameters from the electronic structure calculations of Harding and Klippenstein [30] were used as targets with the uncertainties given in Table 2. The calculations were performed at the MS-CASPT2/CBS//MS-CASPT2/aug-cc-pVDZ (R2), CCSD(T)/CBS//CCSD(T)/aug-cc-pVDZ (R3), MS-CASPT2/CBS//MS-CASPT2/aug-cc-pVTZ (R4), and QCISD(T)/CBS//QCISD(T)/aug-cc-pVTZ (R5) levels of theory. Uncertainties in barrier heights and hindered rotor potentials were assigned concomitant with level of electronic structure theory and level of detail in treatment, respectively. Uncertainties in all other parameters were given estimated typical values. Figure 2 shows the uncertainties in k_4 corresponding to uncertainties in different classes of theoretical kinetics parameters. (Aside from $f_{VRC-TST,c}$, the trends for other reactions are similar.) Rate constant uncertainties are essentially dominated by barrier height uncertainties, especially at low temperatures. The effects of other uncertainties, particularly in harmonic mode frequencies, are more comparable with barrier height uncertainties at higher temperatures. While the total uncertainties in k_4 reach a factor of two to three at 300 K, they are only 50–60% at 2000 K.

3.2. Target class (II): direct rate constant measurements

Rate constant measurements from [17–23,26,42–48] listed in Table 2 were included as targets. Our present choice of uncertainty and weighting factors is motivated by observations that rate constant determination is often subject to higher uncertainties than expected and to systematic errors [34]. Uncertainties for all direct measurements were assigned a factor of two or the scatter in the data, whichever was larger. Weighting factors were taken to be $W_i = 1/N^{0.5}$, where N is the number of points in the data set – equivalent to counting the entire data set as one datum. (As it turns out, reducing all uncertainties by a factor of four reduces constrained k_4 uncertainties substantially but only changes optimized k_4 values by 12%. A more thorough assessment is a nontrivial task that we plan to undertake in future efforts.) Direct measurements of k_1 and k_3 were not included here. Experimental data used to derive k_1 [25,36,37] and k_3 [25] at combustion temperatures were modeled directly as global targets; low-temperature k_3 measurements exhibit pressure dependence [34], which we plan to revisit in a future study.

Figure 3 shows the impact of inclusion of rate constant measurements at low temperatures [17–23] on constraining the uncertainty of the predicted rate constant using *ab initio* targets. The results show that the low-temperature data impose constraints on the kinetics parameters that reduce the propagated uncertainty in high-temperature predicted rate constants substantially. In fact, since the sensitivity of the rate constant to theoretical kinetics parameters is higher at lower temperatures (Fig. 2), a measurement of a given uncertainty at 300 K imposes larger constraints on the model than a corresponding measurement at 2000 K.

3.3. Target classes (III) and (IV): global combustion measurements and experimental conditions

Raw experimental data for global experiments [25,27,36,37] in Table 2 were included as targets. Uncertainties were assigned values as reported, when available. Again, weighting factors were taken to be $W_i = 1/N^{0.5}$. These data include measured OH and/or H_2O time-histories behind reflected shock waves in $H_2O_2/H_2O/O_2/Ar$ (E1–E3) and $H_2O/O_2/Ar$ mixtures (E4) by Hong et al. [27,36,37] and measured absorbance

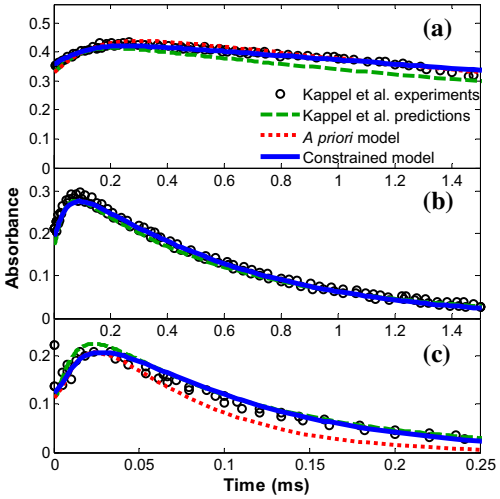

Fig. 5. Absorbance time-histories at 215 nm in shock-heated H_2O_2/Ar mixtures near (a) 968 K and 3.6 atm, (b) 1079 K and 3.4 atm, and (c) 1218 K and 3.0 atm. Symbols represent experimental data from Kappel et al. [25]; lines model predictions.

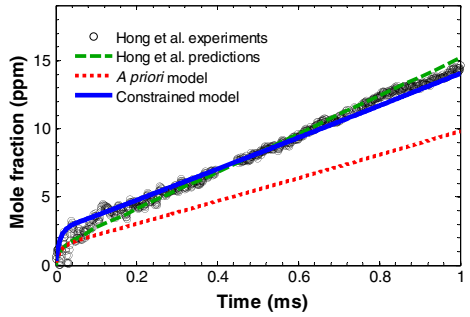

Fig. 6. OH time-histories in shock-heated $H_2O/O_2/Ar$ mixtures near 1880 K and 1.74 atm. Symbols represent experimental data from Hong et al. [27]; lines model predictions.

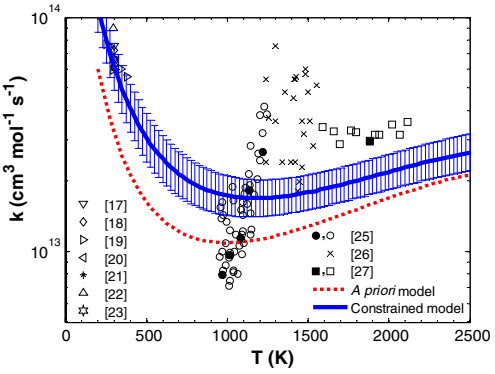

Fig. 7. Selected rate constants for $OH + HO_2 = H_2O + O_2$ (R4). Symbols represent experimental determinations reported in [17–23,25–27] as indicated in the legend. Solid symbols designate experimental determinations reported by Kappel et al. [25] and Hong et al. [27] that correspond to the raw experimental data shown in Figs. 5 and 6 (where the constrained model reproduces the raw data well). Error bars reflect propagated k_4 uncertainties using the constrained model.

time-histories at 215 nm behind reflected shock waves in H_2O_2/Ar mixtures (E5–E9) by Kappel et al. [25]. The absorbance signal [25] at 215 nm includes absorption from both H_2O_2 and HO_2. Experimental condition variables include initial temperatures, T_e, initial pressures, P_e, initial mole fractions, $M_{e,o}$, and parameters describing temperature-dependent absorption cross sections for H_2O_2, $\sigma_{1,H2O2}$ and $\sigma_{2,H2O2}$, and HO_2, $\sigma_{1,HO2}$ and $\sigma_{2,HO2}$, at 215 nm. Uncertainties in σ_{H2O2} and σ_{HO2} were assigned more conservative values than in [25], since σ_{H2O2} was fit to (E5–E9) and σ_{HO2} was extrapolated from lower temperatures. However, the optimized values are within their original estimated uncertainties (~10%).

Conventional A-factor sensitivity analysis of the absorbance signal in shock-heated H_2O_2/Ar mixtures of Kappel et al. [25] (corresponding to Fig. 5a and the apparent rate minimum shown in Fig. 7) reveals high sensitivities to rate constants for R1–R4, with sensitivity coefficients for R2–R4 exhibiting similar trends with time. However, once the constraints imposed by the *ab initio* calculations and uncertainties in the boundary conditions are included, uncertainty-weighted sensitivity analysis reveals minimal contributions from R4 parameters (e.g. see Fig. 4). The prediction uncertainty is essentially dominated by $E^{\dagger}_{(3)}$, k_1, T_5, σ_{H2O2}, and $M_{H2O2,o,5}$ with only minor contributions from R4 parameters – implying that minimal information regarding R4 alone can be directly extracted from the data.

Similar analyses for the OH time-histories in shock-heated $H_2O/O_2/Ar$ mixtures of Hong et al. [27] (corresponding to Fig. 6) reveal $M_{H,o,4}$, $E^{\dagger}_{(4g)}$, T_4, $v_{tr(4g)}$, $\eta_{TS(4g)}$, and $f_{VRC-TST,c(4)}$ as the largest contributors to the overall prediction uncertainty (in descending order) – suggesting that the data provide more direct constraints on R4 parameters but extraction of k_4 is complicated by $M_{H,o,4}$ and T_4 uncertainties.

4. Results and discussion

The set of constrained theoretical kinetics parameters, rate parameters, and experimental condition variables from the present analysis using the targets from Table 2 yield final values and predictions in reasonable consistency with *ab initio* calculations [30], rate constant measurements [17–23,26], and global measurements and experimental conditions [25,27,36,37] used as targets (with all $|Y_{t,i} - F_i(X_{j,opt})| < Z_i$). Constrained variable values and model predictions are provided in the Supplemental data. In particular, as shown below, the optimized model solution is consistent with direct measurements of k_4 at low temperatures, the raw experimental data used to derive k_4 at intermediate to high temperatures, and *ab initio* theoretical kinetics calculations.

Figure 5 shows comparisons of the measured absorbance time-histories in H_2O_2/Ar mixtures behind reflected shock waves [25], predictions using the rate constants originally derived [25], and predictions using the *a priori* and optimized models. The *a priori* model yields reasonable agreement with the experimental data at low temperatures, but it exhibits deficiencies for the higher temperatures. The optimized model shows significant improvements – reproducing the raw experimental data better than the rate constants derived originally [25]. The largest differences between the constrained model and the original interpretations appear to be rate constants for the other reactions. In fact, when k_4 is re-derived from the k_4/k_2 values from [25] using the optimized k_2, the pronounced "well" essentially disappears. Therefore, the

apparent anomalous temperature dependence of k_4 appears to be primarily attributable to previous uncertainties in k_2, for which highly constraining data have become available recently [37] (included here as targets).

Figure 6 shows comparisons of the measured OH time-histories in $H_2O/O_2/Ar$ mixtures behind reflected shock waves [27], predictions originally used to derive k_4 [27], and predictions using the *a priori* and optimized model. Similar to the results for Fig. 5, the optimized model shows significant improvements over the *a priori* model – reproducing the experimental data equally as well as the prediction used to derive k_4 originally [27] with a 70% higher $M_{H,o,4}$ (an arbitrary fitting parameter [27]), 0.25% higher T_4, and 40% lower k_4.

Figure 7 shows comparisons of k_4 determinations from [17–23,26] (treated as direct rate constant measurements), k_4 determinations from [25,27] (treated as global experiments, see Figs. 5 and 6), and the *a priori* and optimized k_4 values calculated from the theoretical kinetics variables. The k_4 values using the optimized model are higher than the *a priori* model values by about a factor of two at 300 K and 30% at 2000 K – yielding closer values to k_4 determinations of [17–23,26]. While the optimized k_4 expression shows a much less pronounced temperature dependence than the k_4 values derived by Kappel et al. [25] and somewhat lower k_4 values than derived by Hong et al. [27], the optimized model that uses this k_4 expression reproduces the raw experimental data from both studies equally as well as (and in some cases better than) the modeling performed by the original authors (see Figs. 5 and 6).

Simultaneous weighting of multiple sources of information, as performed here, discriminates among otherwise indistinguishable sets of co-dependent parameters (as in rate constants for data in Fig. 5 and initial conditions in Fig. 6). Clearly, raw data and careful documentation as made available by Kappel et al. [25] and Hong et al. [27] are extremely powerful. They enable later reinterpretation of valuable data in the presence of new information and new modeling techniques. The present demonstration appears to be a particularly compelling example of the inherent value of including raw data in journal submissions and/or community databases to ensure maximum impact of the work in the future.

5. Conclusions

A framework for combustion model development that encapsulates behavior across a wide range of chemically relevant scales from fundamental molecular interactions to global combustion phenomena is presented. The multi-scale approach enables self-consistent use of information from a variety of data sources and reliable extrapolation beyond available data at limited temperature/pressure/bath-gas conditions. Implementation for the H_2O_2 decomposition mechanism yields an optimized model that is consistent with *ab initio* calculations and experimental data for $OH + HO_2 = H_2O + O_2$ across the entire temperature range, including those that indicated a peculiar, deep rate minimum near 1000 K. In contrast, the present expression exhibits much weaker temperature dependence, with a shallow minimum typical of reactions with submerged barriers [50].

The optimized rate constant is well represented from 200–3000 K (within 5%) by the bi-Arrhenius expression:

$$k_4(T) = 1.93 \times 10^{20} T^{-2.49} \exp(-294K/T) + 1.21 \times 10^{9} T^{1.24} \exp(658K/T) \ [\mathrm{cm^3\ mol^{-1}\ s^{-1}}]$$

Recent k_4 experiments near 1000–1300 K [51], of which we became aware after submission of this paper, are in remarkable agreement with the present results.

Acknowledgements

This work was supported by a Director's Postdoctoral Fellowship from Argonne National Lab and by the U.S. Department of Energy, Office of Basic Energy Sciences, Division of Chemical Sciences, Geosciences, and Biosciences, under Contract No. DE-AC02-06CH11357. The authors would also like to thank Dr. Zekai Hong for providing the raw data from [27,36,37].

Appendix A. Supplementary data

Supplementary data associated with this article can be found, in the online version, at http://dx.doi.org/10.1016/j.proci.2012.05.041.

References

[1] W. Hwang, J. Dec, M. Sjöberg, *Combust. Flame* 154 (2008) 387–409.
[2] R. Sivaramakrishnan, A. Comandini, R.S. Tranter, K. Brezinsky, S.G. Davis, H. Wang, *Proc. Combust. Inst.* 31 (2007) 429–437.
[3] M.P. Burke, M. Chaos, F.L. Dryer, Y. Ju, *Combust. Flame* 157 (2010) 618–631.
[4] C.K. Westbrook, F.L. Dryer, *Prog. Energy Combust. Sci.* 10 (1984) 1–57.
[5] M. Frenklach, *Combust. Flame* 58 (1984) 69–72.
[6] M. Frenklach, H. Wang, M.F. Rabinowitz, *Prog. Energy Combust. Sci.* 18 (1992) 47–73.
[7] G.P. Smith, D.M. Golden, M. Frenklach, et al., GRI-MECH 3.0, 1999, available at http://www.me.berkeley.edu/gri_mech/.
[8] M. Frenklach, A. Packard, P. Seiler, R. Feeley, *Int. J. Chem. Kinet.* 36 (2004) 57–66.

[9] D. Sheen, X. You, H. Wang, T. Lovas, *Proc. Combust. Inst.* 32 (2009) 535–542.
[10] T. Nagy, T. Turányi, *Int. J. Chem. Kinet.* 43 (2011) 359–378.
[11] T. Turányi, T. Nagy, I.Gy. Zsély, et al., *Int. J. Chem. Kinet.* 44 (2012) 284–302.
[12] D.M. Golden, G.P. Smith, A.B. McEwen, et al., *J. Phys. Chem. A* 102 (1998) 8598–8606.
[13] H. Huang, D.J. Merthe, J. Zádor, L.E. Jusinski, C.A. Taatjes, *Proc. Combust. Inst.* 33 (2011) 293–299.
[14] M.P. Burke, M. Chaos, Y. Ju, F.L. Dryer, S.J. Klippenstein, *Int. J. Chem. Kinet.* 44 (2012) 444–474.
[15] M.P. Burke, F.L. Dryer, Y. Ju, *Proc. Combust. Inst.* 33 (2011) 905–912.
[16] S.J. Klippenstein, L.B. Harding, M.J. Davis, A.S. Tomlin, R.T. Skodje, *Proc. Combust. Inst.* 33 (2011) 351–357.
[17] W.B. DeMore, *J. Phys. Chem.* 83 (1979) 1113–1118.
[18] W.B. DeMore, *J. Phys. Chem.* 86 (1982) 121–126.
[19] L.F. Keyser, *J. Phys. Chem.* 92 (1988) 1193–1200.
[20] R.R. Lii, R.A. Corse, M.C. Sauer, S. Gordon, *J. Phys. Chem.* 84 (1980) 813–817.
[21] R.A. Cox, J.P. Burrows, T.J. Wallington, *Chem. Phys. Lett.* 84 (1981) 217–221.
[22] M.J. Kurylo, O. Klais, A.H. Laufer, *J. Phys. Chem.* 85 (1981) 3674–3678.
[23] M. Braun, A. Hofzumahaus, F. Stuhl, *Ber. Bunsenges Phys. Chem.* 86 (1982) 597–602.
[24] H. Hippler, H. Neunaber, J. Troe, *J. Chem. Phys.* 103 (1995) 3510–3516.
[25] Ch. Kappel, K. Luther, J. Troe, *Phys. Chem. Chem. Phys.* 4 (2002) 4392–4398.
[26] N.K. Srinivasan, M.C. Su, J.W. Sutherland, J.V. Michael, B. Ruscic, *J. Phys. Chem. A* 110 (2006) 6602–6607.
[27] Z. Hong, S. S Vasu, D.F. Davidson, R.K. Hanson, *J. Phys. Chem. A* 114 (2010) 5520–5525.
[28] M. Chaos, F.L. Dryer, *Combust. Sci. Technol.* 180 (2008) 1053–1096.
[29] C.L. Rasmussen, J. Hansen, P. Marshall, P. Glarborg, *Int. J. Chem. Kinet.* 40 (2008) 454–480.
[30] L.B. Harding, S.J. Klippenstein, unpublished.
[31] D.A. Sheen, H. Wang, *Combust. Flame* 158 (2011) 645–656.
[32] B. Ruscic, R.E. Pinzon, M.L. Morton, et al., *J. Phys. Chem. A* 108 (2004) 9979–9997.
[33] M.J. Davis, R.T. Skodje, A.S. Tomlin, *J. Phys. Chem. A* 115 (2011) 1556–1578.
[34] D.L. Baulch, C.T. Bowman, C.J. Cobos, et al., *J. Phys. Chem. Ref. Data* 34 (2005) 757–1397.
[35] K. Miki, S.H. Cheung, E.E. Prudencio, P.L. Varghese, in: 7th International Conference on Chemical Kinetics, Massuchussets Institute of Technology, Cambridge, MA, July 10–14, 2011.
[36] Z. Hong, A. Farooq, E.A. Barbour, D. F Davidson, R.K. Hanson, *J. Phys. Chem. A* 113 (2009) 12919–12925.
[37] Z. Hong, R.D. Cook, D. F Davidson, R.K. Hanson, *J. Phys. Chem. A* 114 (2010) 5718–5727.
[38] D.G. Truhlar, B.C. Garrett, S.J. Klippenstein, *J. Phys. Chem. A* 100 (1996) 12771–12800.
[39] S.J. Klippenstein, A.F. Wagner, R.C. Dunbar, D.M. Wardlaw, S.H. Robertson, J.A. Miller, VARIFLEX, version 1.14m; 2005.
[40] Y. Georgievskii, S.J. Klippenstein, *J. Phys. Chem. A* 111 (2007) 3802–3811.
[41] A.E. Lutz, R.J. Kee, J.A. Miller, Report SAND-87-8248 Sandia National Laboratories, Albuquerque, NM, 1988.
[42] U.C. Sridharan, B. Reimann, F. Kaufman, *J. Chem. Phys.* 73 (1980) 1286–1293.
[43] L.F. Keyser, *J. Phys. Chem.* 84 (1980) 1659–1663.
[44] M.K. Bahng, R.G. Macdonald, *J. Phys. Chem. A* 111 (2007) 3850–3861.
[45] Y. Bedjanian, G. Le Bras, G. Poulet, *J. Phys. Chem. A* 103 (1999) 7017–7025.
[46] M.S. Wooldridge, R.K. Hanson, C.T. Bowman, *Int. J. Chem. Kinet.* 26 (1994) 389–401.
[47] J.W. Sutherland, P.M. Patterson, R.B. Klemm, *Proc. Combust. Inst.* 23 (1990) 51–57.
[48] A. Lifshitz, J.V. Michael, *Proc. Combust. Inst.* 23 (1990) 59–67.
[49] E. Goos, A. Burcat, B. Ruscic, *Third Millennium Ideal Gas and Condensed Phase Thermodynamical Database for Combustion with Updates from Active Thermodynamical Tables*, ANL-05/20 and TAE 960 Technion-IIT, Aerospeace Engineering, and Argonne National Laboratory, Chemistry Division, September 2005, available at <ftp://ftp.technion.ac.il/pub/supported/aetdd/thermodynamics/therm.dat>; (accessed August 2011).
[50] H. Sabbah, L. Biennier, I.R. Sims, Y. Georgievskii, S.J. Klippenstein, I.W.M. Smith, *Science* 5834 (2007) 102–105.
[51] Z. Hong, K.-Y. Lam, R. Sur, S. Wang, D.F. Davidson, R.K. Hanson, *Proc. Comb. Inst.* (2012), in press.